



NEW NANOSIZED SYSTEMS WITH ANTITUMOR ACTIVITY BASED ON THE Pt(IV) COMPLEXES WITH NICOTINAMIDE LIGANDS AND AMPHIPHILIC COPOLYMERS OF N-VINYLPYRROLIDONE AND (DI)METHACRYLATE

Cite this: *INEOS OPEN*, **2021**, 4 (5), 195–201
DOI: 10.32931/io2123a

S. V. Kurmaz,^a D. V. Konev,^a V. A. Kurmaz,^{*a} G. I. Kozub,^a
V. M. Ignat'ev,^{a,b} N. S. Emel'yanova,^a A. A. Balakina,^a and A. A. Terentyev^a

Received 2 December 2021,
Accepted 19 January 2022

^a Institute of Problems of Chemical Physics, Russian Academy of Sciences,
pr. Akademika Semenova 1, Chernogolovka, Moscow Oblast, 142432 Russia
^b Department of Physical and Chemical Engineering, Lomonosov Moscow State
University, Leninskie Gory 1, str. 51, Moscow, 119991 Russia

http://ineosopen.org

Abstract

The nanosized systems involving Pt(IV) complexes with antitumor activity are obtained by their solubilization via amphiphilic copolymers of *N*-vinylpyrrolidone and (di)methacrylates synthesized by the radical copolymerization in toluene without any polymer chain growth terminating agents. The resulting systems are investigated by a complex of physico-chemical methods (IR spectroscopy, DLS, TEM, cyclic and square-wave voltammetry) and quantum chemical simulation. The Pt(IV) complexes are shown to have cytotoxic effects on A-172 tumor cells and the corresponding cytotoxicity indices (IC₅₀) are determined. The amphiphilic copolymers under consideration are promising modern platforms and delivery vehicles for biologically active compounds.

Key words: amphiphilic copolymers, *N*-vinylpyrrolidone, dimethacrylate, Pt(IV) complexes, encapsulation, cytotoxicity.

Introduction

The discovery of cisplatin in the 1960s [1] prompted the development of a broad class of platinum compounds as potential antitumor agents. Nowadays, Pt(II) complexes such as cisplatin, carboplatin, and oxaliplatin are successfully utilized in medical practice among the drugs with high antimetastatic activity [2–4]. However, their applicability is restricted by rather high overall toxicity and low selectivity. Therefore, an important challenge is to produce platinum tetrachloride complexes with low-toxic biogenic ligands, *e.g.*, nicotinic or isonicotinic acids and their derivatives [5, 6]. Several Pt(IV) complexes bearing different aminonitroxyl derivatives as ligands [7, 8] have been synthesized and studied for cytotoxicity and antitumor activity [9]. They were introduced into various carriers *via* encapsulation, covalent or complexation/coordination binding to tune the properties of the platinum complexes such as solubility, bioavailability, prolonged action, distribution in the body, duration of circulation in the blood, accumulation in tumors and foci of inflammation, toxicity, *etc.* [10]. Natural cavitands like cucurbiturils [11] or different biocompatible and biodegradable copolymers [12] can serve as carriers for platinum-based drugs. Dendrimers are also considered promising delivery systems owing to their three-dimensional globular structure, nanoscale sizes, monodispersity, lipophilicity, and the ability to easily penetrate cells [13–16]. However, their synthesis often represents multistep processes. In addition, some of them, for example, the dendrimers with primary amino groups and a positively charged shell exhibit high cell toxicity [17]. Despite

the architectural irregularity and imperfection, branched amphiphilic polymers may represent an alternative to them. Earlier, we have proposed to encapsulate organic platinum(IV) complexes (PC) featuring antitumor activity into amphiphilic copolymers of *N*-vinylpyrrolidone (VP) and triethylene glycol dimethacrylate (TEGDM) with branches in chains [18–20]. The goal of this work was to obtain and characterize the nanoscale systems of Pt(IV) complexes with biogenic ligands based on a new generation of amphiphilic VP copolymers (Fig. 1) and to study their cytotoxicity against A-172 tumor cells.

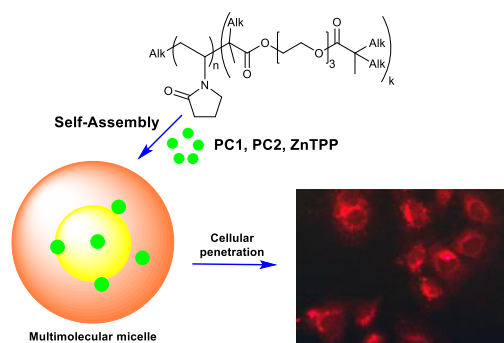


Figure 1. Chemical structure of the VP-TEGDM branched copolymer.

Results and discussion

This investigation was concerned with *cis*-bis-[nitroxyethyl isonicotinamide-*N*]tetrachloride platinum(IV) (PC1) and *cis*-bis-[nitroxyethylisonicotinamide-*N*]tetrachloride platinum(IV), (PC2) [5, 6]. Their chemical structures are presented in Fig. 2.

Characterization of the copolymers

The amphiphilic copolymers VP-TEGDM and VP-TEGDM containing poly(ethylene glycol) methyl ether methacrylate (PEGM) units of different monomer compositions and molecu-

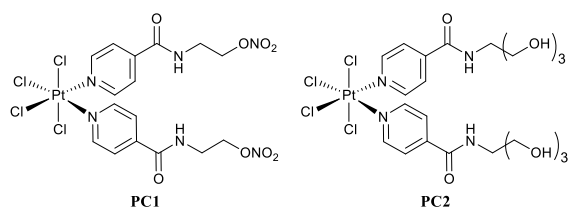


Figure 2. Platinum(IV) complexes **PC1** and **PC2**.

lar masses obtained with the monomer admixture at 100/5 (**A**, **B**), 95/5/5 and 98/2/5 (**C**, **D**) molar ratios were used as the carriers. Copolymers **A** and **B** represented the fractions soluble and insoluble in toluene, respectively. The copolymers considerably differed in the monomer compositions, molecular masses, and topological structures. The contents of (di)methacrylate units in **A**, **B**, **C**, and **D** were 5.4, 19.6, 11.8, and 9.3 mol %, respectively. Their absolute molecular masses (M_w) were 26, 196, 350, and 120 kDa, respectively. Depending on the concentration, the amphiphilic VP copolymers exist in alcohols and water as separated macromolecules of a micellar type and/or their aggregates, namely, multimolecular micelles with hydrodynamic radii (R_h) of ~4 and 30–90 nm, respectively. Copolymers **A** and **B** are thermosensitive, while copolymers **C**, **D** respond little to the temperature changes as a result of the presence of the PEGM units in the polymer chains and a shift of the lower critical solution temperature to higher values.

Calculations

The Pt(IV) complexes were encapsulated into the polymer particles, such as monomolecular polymer micelles and/or their aggregates, using the solutions of the copolymers in *i*-PrOH and the PC solutions in biocompatible DMSO [18, 19]. Isopropyl alcohol is a thermodynamically unsuitable solvent for platinum complexes, as well as water, by the way. They stimulate their inclusion into the polymer particles and the formation of nanostructures in which the guest molecules form hydrogen bonds with the electron-donor copolymer groups.

According to the results of quantum chemical calculations, **PC1** is connected to VP-VP-VP units of the copolymer primarily through the hydrogen atom of the amide group (Fig. 3, **pta1**, **ptb2**, and **ptb3**). The hydrogen bond donors can be both the oxygen atoms of the lactam ring (**pta1**) and those of the TEGDM units (**ptb2**, **ptb3**). However, **pta3** structure in which the hydrogen atoms of the alkyl groups act as hydrogen bond donors is also possible.

The parameters of hydrogen bonds in the PC–copolymer structures are given in Table 1. According to the hydrogen bond formation criterion [21], the electron density value (ρ) and its Laplacian ($\nabla^2\rho$) should be within 0.002–0.040 and 0.024–0.139, respectively. The majority of the considered bonds fell just in this range. The exclusions are bonds in **pta1** and **pta3**.

The bonds formed in **pta1** complex have higher ρ and $\nabla^2\rho$ values, which indicates their partially covalent character. Bonds formed in **pta3** have lower ρ and $\nabla^2\rho$ values, which can evidence a higher van der Waals contribution to this type of bonding. The bond energy (E_{bond}) reduces along with ρ and $\nabla^2\rho$ but one should keep in mind their cooperative character. The total energy of bonds presented in **pta3** is equal to 10.1 kcal/mol. This suggests that **PC1** can bind with the VP copolymers also through the alkyl hydrogen atoms.

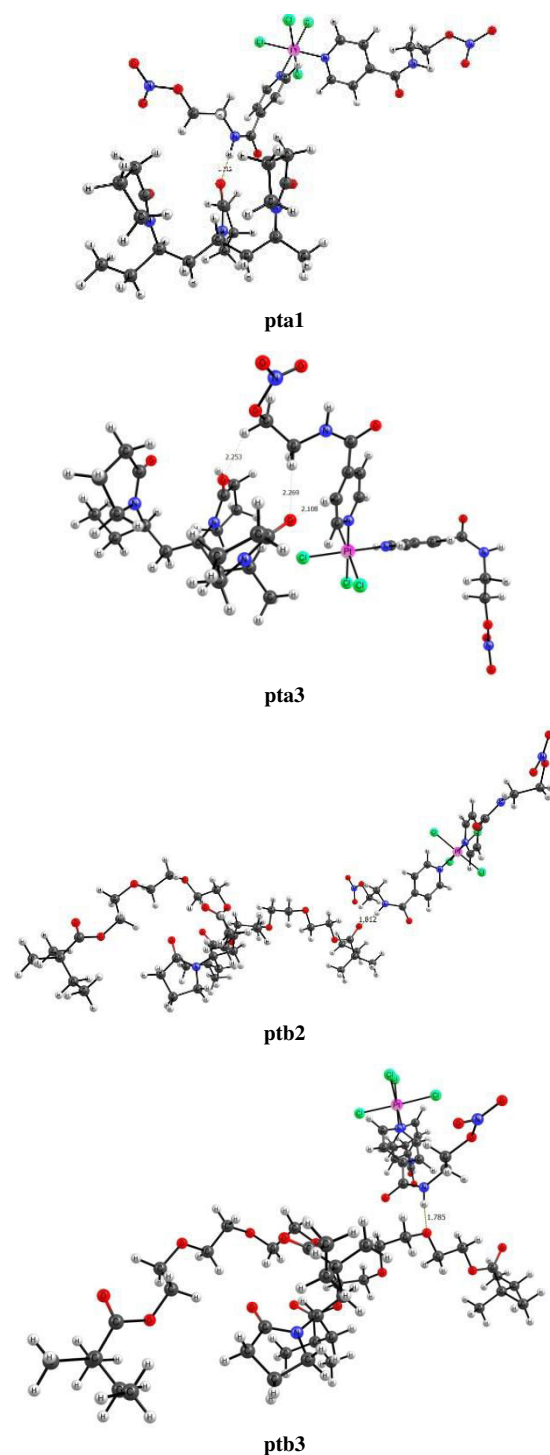


Figure 3. Structures of the H-complexes formed between **PC1** and the copolymer site consisting of VP-VP-VP units.

Table 1. Hydrogen bond parameters in the PC–copolymer structures

Structure	ρ , a.u.	$\nabla^2\rho$, a.u.	E_{bond} , kcal/mol
pta1	0.044452	0.157642	13.3
pta3	0.016093	0.079179	4.2
	0.013652	0.059365	3.0
	0.012939	0.055573	2.9
ptb2	0.031589	0.134589	9.6
ptb3	0.038302	0.138709	11.2
pta1l	0.039115	0.143956	11.6
	0.013203	0.061685	3.1
pta2l	0.060023	0.191581	19.6

The **PC2** complexes with a VP-VP-VP site of the VP-TEGDM copolymer were also considered. **PC2** was found to be bonded in these systems like in the previous case through the hydrogen atoms of the amide and alkyl groups. The hydrogen atom of the hydroxy group can also act as a hydrogen bond donor (Fig. 4).

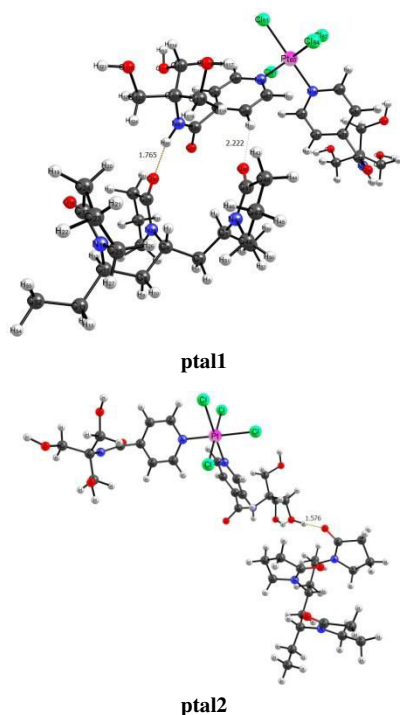


Figure 4. Structures of complexes **ptal1** and **ptal2**.

It should be noted that bonds in **ptal1** do not differ in characteristics from the analogous bonds in **pta1** and **pta3** (Table 1). In complex **ptal2**, the hydrogen atom of the hydroxy group acts as a hydrogen bond donor. It is sufficiently stronger than other hydrogen bonds if considering the parameters that affect the bonding force: ρ , $\nabla^2\rho$, and E_{bond} . As well as in complex **pta1**, this is indicative of the partially covalent character and suggests that the **PC2** complexes with the VP copolymers can be more stable in aqueous solutions than those of **PC1**.

Properties of the copolymer compositions with the platinum(IV) complexes

Figure 5 shows the transmission electron microscopy (TEM) images of **PC1-B** and **PC1-C** structures. Their morphologies differ and depend on the type of the copolymer carrier.

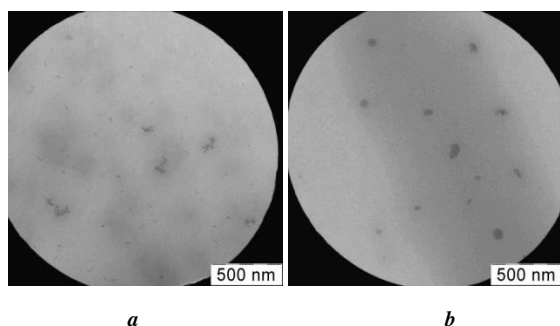


Figure 5. TEM images of **PC1-B** (a) and **PC1-C** (b) nanostructures.

The distribution of the intensity of light scattering for a neutral aqueous phosphate buffer solution (PBS, pH 6.8) by particle sizes is polymodal but becomes narrower and is unimodal for **PC1-B** with a temperature rise (Fig. 6a) [19]. In this case, the value of R_h for scattering centers is ~ 50 nm at the peak maximum. The intensity of light scattering for the **PC1-A** and **PC1-B** aqueous buffer solutions increases significantly with temperature, while that for **PC1-C** practically does not change. Thus, the nanosized systems based on the VP-TEGDM copolymers are thermosensitive and the release of an active substance from the polymer particles can be expected under the temperature effect.

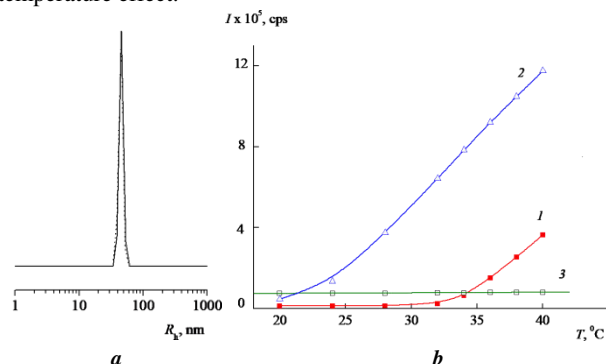


Figure 6. Numerical size distribution of **PC1-B** particles at 38 °C (a) and the temperature dependences of the intensity of light scattering (b) for aqueous neutral buffer solutions of **PC1-A** (1), **PC1-B** (2), and **PC1-C** (3) (composite concentrations: 1.4, 1.8, and 1.4 mg/mL, respectively).

The experimental contents of Pt ($\sim 4\%$) and Cl ($\sim 4\%$) in **PC1** encapsulated into copolymer A satisfactorily coincide with the theoretical values. This indicates the stability of **PC1** during the formation of the polymer composition. The metal coordination sphere and metal–ligand bonding character in **PC2** encapsulated into copolymer C are retained, which is evidenced by the characteristic absorption band at ~ 350 cm^{-1} in the IR spectrum (Fig. 7).

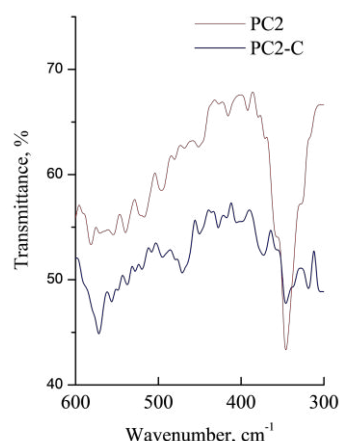


Figure 7. IR spectra of free **PC2** and the complex encapsulated into copolymer C within the range of 600–300 cm^{-1} .

The IR spectroscopic analysis of **PC1-C** powder (Fig. 8) has revealed that the intensity of characteristic absorption of water involved in the formation of a hydrogen bond with the copolymer at 3600–3000 cm^{-1} significantly reduces compared to that of the initial copolymer [19]. At the same time, the absorption band corresponding to the stretching vibrations of the

lactam C=O groups is shifted to higher wavenumbers from 1655 to 1665 cm^{-1} . This testifies the formation of a hydrogen bond between the C=O group of the copolymer VP units and the N–H group of **PC1** complex.

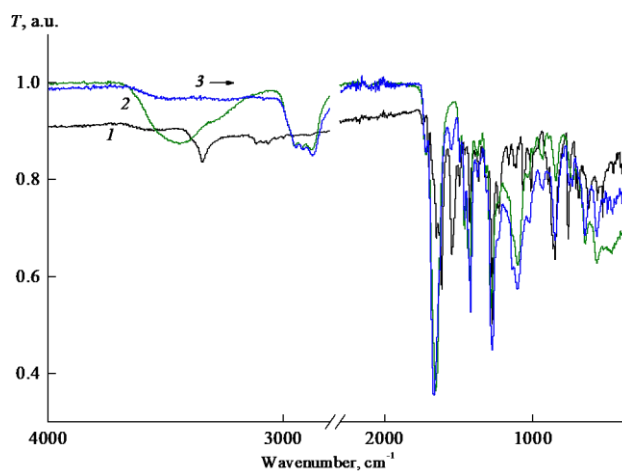


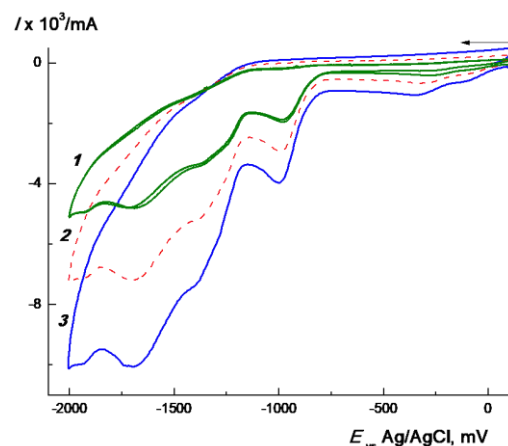
Figure 8. IR spectra of the powder samples of **PC1** (1), copolymer C (2), and **PC1**–C composition (3).

The cyclic voltammetry (CVA) data obtained on a glassy carbon electrode (GC) independently confirm the involvement of **PC1** in copolymer C. The CVA curves of the polymer particles loaded with **PC1** in PBS and DMSO are quite different (*cf.* Figs. 9a and 9b). Thus, only two poorly defined overlapped peaks are observed in the first case until $E \sim -1.6$ V (Fig. 9b), and no other peaks are observed until these potentials. Earlier we have already observed considerable differences in the electrochemical behavior between the initial forms of depolarisers and those encapsulated into the related copolymers, *e.g.*, in the case of zinc tetraphenylporphyrinate (ZnTPP) [22] and Rose Bengal [23].

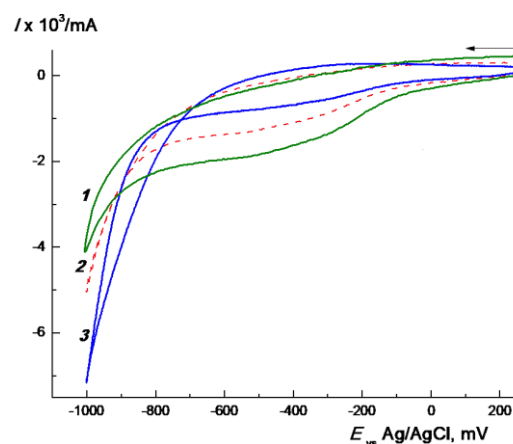
However, the CVA curves of the polymer particles loaded with this Pt(IV) complex in DMSO are complicated and contain 4 to 5 cathodic peaks within the potential range of $-(0.2-1.6)$ V like for the free complex (Fig. 9c). Evidently, the **PC1**–copolymer structures decompose in this solution as, for example, the copolymer structures of other nature loaded with ZnTPP in MeCN [22]. As a result, free complex **PC1** is released and reduced irreversibly. Furthermore, DMSO is well known as a solvent with a sufficiently high coordinating ability. It can interact with highly reactive intermediates to form an ecologically hazardous methyl radical [24]. Therefore, we used additionally MeCN as a much more stable and non-coordinating solvent, although the solubility of **PC1** in it could be insufficient [5, 6].

In general, the electrochemical data of Pt(IV) complexes, in particular, the reduction potentials usually correlate with their antitumor activity, although such a correlation is not always evident and unambiguous [25, 26]. However, a correlation between the cytotoxic activity and the standard potential of a redox-peak E^0 of a drug was found [27].

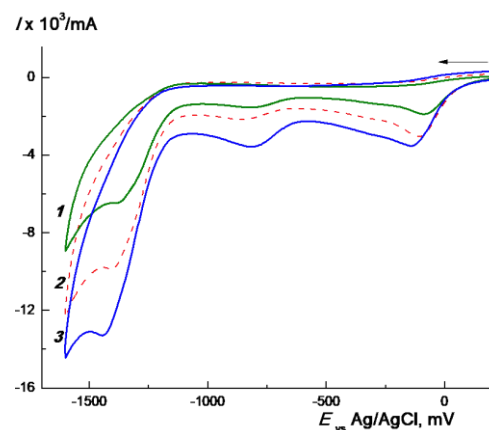
PC1 demonstrates somewhat more complicated behavior in MeCN (Fig. 10a). The corresponding CVA curves, in general, resemble those shown in Fig. 9c for DMSO solution but noticeably differ quantitatively. Like in the case of DMSO, 4 to 5 poorly defined, partially overlapped irreversible reduction



a



b



c

Figure 9. CVA curves recorded on a GC electrode at different scan rates for **PC1** encapsulated into copolymer C (a, b) and free complex **PC1** (c) [19]: DMSO + 0.1M TBAPF₆ (a), aqueous phosphate buffer solution + 0.5 KCl (b), 0.0016M **PC1** in DMSO + 0.1M TBAPF₆ (c). Scan rates v , $\text{mV}\cdot\text{s}^{-1}$: 20 (1), 50 (2), 100 (3).

waves can be distinguished on the CVA curve registered in MeCN. At the same time, the first two waves are separated more clearly. This is more evident from the square-wave voltammetry (SWVA) curves obtained under the same conditions (*cf.* Fig. 9a and 10). Probably, such behavior is associated with the differences in nature and rates of subsequent chemical stages of the conversion of intermediates. An oxidation wave at about

+0.2 V appears on a reverse scan, which is much less pronounced in DMSO. However, the main difference is that the solubility of **PC1** in MeCN indeed appeared to be considerably lower, at least, by an order of magnitude than that in DMSO. This can lead to the formation of a deposit on the electrode and, as a result, the appearance of various distortions on the CVA curves. Therefore, thorough purification of the electrode surface after each measurement in MeCN is strongly required. Kinks as before –1 V or slow decrease like after –1.2 V (Figs. 9c and 10a) are observed usually when a current on the initial part of CVA curves has a diffusion character and is controlled by kinetics on their decrease [28]. Such a behavior could be observed often in organic electrochemistry, for example, during the reduction of cinnamic acid on a carbosital electrode [29]. We used SWVA to visualize the differences in the electrochemical behavior of **PC1** in DMSO and MeCN. The remarkable differences (namely, two well-defined peaks and three kinks in DMSO together with five well-defined peaks and one kink in MeCN) (Fig. 10b) could indicate some differences in the mechanism of **PC1** electrode reactions in these solvents and/or different stabilities of the intermediates. This can originate from a big difference in the coordination properties of strongly coordinating DMSO and poorly coordinating MeCN.

In general, such a high electrochemical activity of the Pt(IV) complexes allows for expecting the high antitumor activity [27].

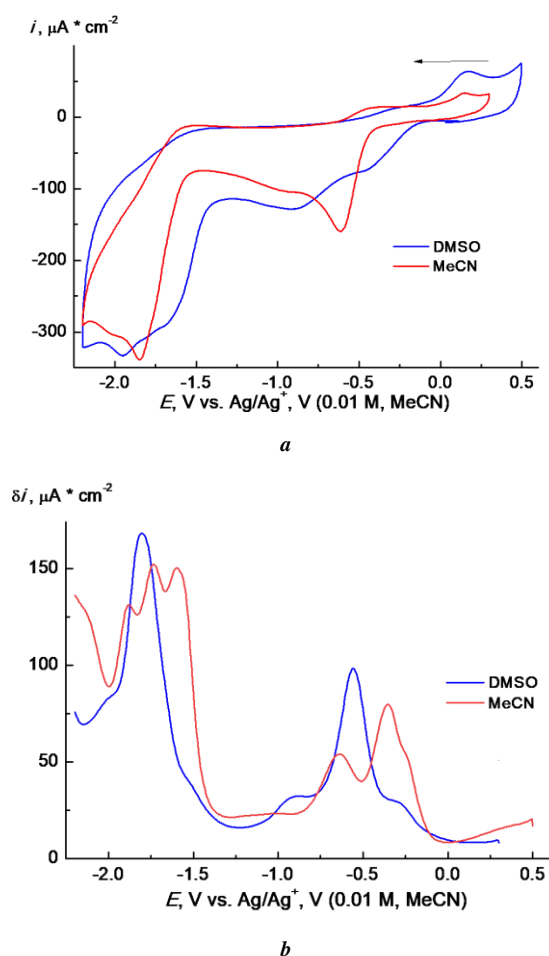


Figure 10. CVA curves (a) for **PC1** + 0.1M TBAPF₆ recorded on a GC electrode in MeCN (0.0006M of **PC1**, blue solid line) and DMSO (0.0012M of **PC1**, red dashed line) at 100 mV·s⁻¹, the first scan; SWVA curves (b) of the same solutions.

Cytotoxicity of the Pt(IV)C nanosized systems

Copolymers **A–D** were shown to have no significant effect on the viability of model tumor cells HeLa (human cervical carcinoma) and A-172 (human glioblastoma), as well as normal Vero cells derived from monkey kidney in the concentration range from 7 to 700 µg·mL⁻¹. The choice of HeLa cells that mimic the human body *in vitro* was dictated by their known ability to endlessly divide, simplicity during cultivation, freezing and conservation, as well as good reproducibility of research results. The dependences of MTT staining on the concentration of free **PC1** and the complex encapsulated into copolymers **A–C** confirm their cytotoxicity against A-172 cells. The IC₅₀ value for **PC1** was ca. 90.6 µM after 48 h of incubation. The IC₅₀ rates for **PC1** encapsulated into copolymers **A–D** were about 106 µM.

To visualize the penetration of the polymer particles into cells, the nanosized systems based on copolymer **D** and ZnTPP were produced (Fig. 11). Rather weak overlapping staining of nuclei (DAPI) and nanoparticles indicates their localization in the cell cytoplasm. The number of Vero and HeLa cells with double staining was as high as 97.0 ± 2.5 and 99.4 ± 0.7%, respectively. Therefore, the polymer nanoparticles can efficiently accumulate in cells and provide intracellular delivery of a biologically active substance.

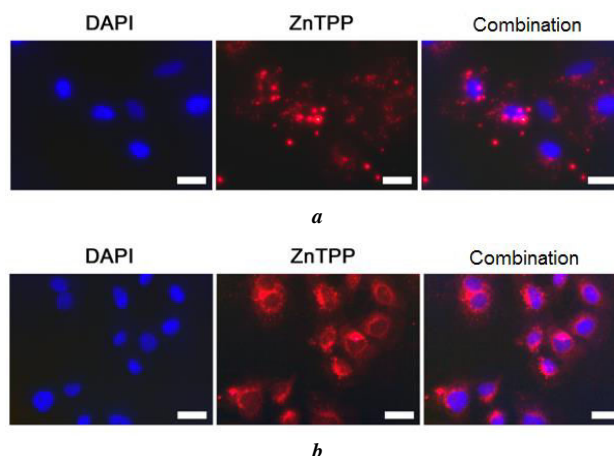


Figure 11. Fluorescence microscopy images of Vero (a) and HeLa (b) cells after 24 h of incubation in the presence of the copolymer **D** nanoparticles loaded with ZnTPP. The scale bar is 20 µm.

Experiment and calculations

Cis-bis-[nitroxyethyl isonicotinamide-*N*]tetrachloride platinum(IV) (**PC1**) and *cis*-bis-[*N*-nicotinoyltrimethylolmethane-*N*]tetrachloride platinum(IV) (**PC2**) were synthesized by the reactions of K₂[PtCl₆] with *N*-(2-nitroxyethyl isonicotinamide or hexachloroplatinic acid with *N*-nicotinoyltri(hydroxymethyl)aminomethane [5, 6]. The platinum and chlorine contents in the encapsulated complex (11% per copolymer **A**) were determined using Pregl's chemical analysis and mercurimetric titration, respectively [19].

To obtain the copolymers, VP (Alfa Aesar, USA) was purified by vacuum distillation to remove NaOH inhibitor. Triethylene glycol dimethacrylate (TEGDM) and poly(ethylene glycol) methyl ether methacrylate (PEGMEM) (Aldrich) were used as received without additional purification. MeCN (Lab-Scan, Poland), *i*-PrOH (extra pure), and the components of

neutral phosphate buffer (pH 6.8) solutions, *i.e.*, NaCl, KCl, Na₂HPO₄, and KH₂PO₄ (all obtained from Khimmed, Russia) were also used as purchased. Bu₄NPF₆ (TBAPF₆) (Fluka, >99%) was kept before the experiment in an oven at 80 °C for a day. DMSO (Lab-Scan, HPLC gradient grade, Poland) was purified by freezing; the water content in it (no more than 0.05%) was controlled by IR spectroscopy according to the published procedure [30].

The amphiphilic VP copolymers were obtained by the radical copolymerization in toluene without any polymer chain growth terminating agents [18, 19].

The DLS measurements for aqueous neutral PBS solutions (pH = 6.8) of the PC-copolymer structures were carried out at the detection angle of 90° using a Photocor Compact unit (Photocor Instruments Inc., USA) equipped with a diode laser operating at the wavelength of 654 nm. The experimental data were processed using DynaLS v. 2.8.3 software. The FTIR spectra were recorded on a Bruker ALPHA FTIR spectrophotometer in the range of 4000–400 cm⁻¹ (number of scans 16) and a Specord M80 spectrophotometer (powder samples or KBr pellets). The CHN contents were analyzed on a Vario cube instrument (Elementar GmbH). The absolute molecular weights of the copolymers were determined using an HPLC Waters GPCV 2000 chromatograph (2 columns PS-gel, 5 microns, MIXED-C, 300 × 7.5 mm) equipped with a WYATT DAWN HELEOS II (658 nm) refractometric and light scattering detector in *N*-methylpyrrolidone in the presence of LiCl (1%) in order to avoid the aggregation of macromolecules. The aqueous solution of the PC composition was applied to the substrate, water was quickly evaporated, and an image was obtained with a Leo 912 AB unit (Leo Electron, Carl Zeiss AG, Hsu Koehn, Germany).

The electrochemical experiments were carried out in three-electrode 10 cm³ quartz and glass cells without separation of the cathodic and anodic areas *via* cyclic voltammetry with an IPC-ProL potentiostat (IPCE RAS, Russia) and an Autolab/PGSTAT302N universal high-speed potentiostat/galvanostat (ECOCHEMIE, Netherlands). The rate of the potential scan range was 0.01–1 V·s⁻¹; in the SWVA experiments, the potential step was 5 mV, the amplitude was 20 mV, and the frequency was 25 Hz. The working electrodes were a GC disc electrode with a diameter of 1.6 mm polymerized into an inert PEEK polymer (AES, Japan) and an HTW Segradur-G electrode (Germany) soldered into a glass diameter of ~1 and 3 mm², respectively. The auxiliary electrode was a Pt wire, and the reference electrode was a silver/silver chloride electrode (Ag/AgCl) in aqueous solutions. The measurements in non-aqueous solutions were carried out relative to the Ag/Ag⁺ reference electrode (10 mmol·L⁻¹ of AgNO₃, 100 mmol·L⁻¹ of Bu₄NPF₆ in the used solvent, *i.e.*, MeCN or DMSO) separated from the working compartment of the cell by a double porous glass diaphragm. Its potential was +300 mV vs Ag/AgCl.

The GC electrode was polished immediately before an experiment by a diamond suspension (diameter of 1 μm) and then rinsed with ultrasonic machining in a media where the investigation was performed (water or the corresponding organic solvent). Before the experiments, the working solutions were deaerated by alternately applying a vacuum and filling the electrochemical cells with argon. When the components of the working solution and electrodes were introduced into the cell

and during the electrochemical measurements, a slight excess argon pressure (~20 mbar) was maintained above the solutions. The standard Schlenk procedure [18, 31, 32] was used for the experiments. A detailed description of the CVA experiments can be found elsewhere [18, 19, 22, 23, 31].

The structures of the H-complexes formed by **PC1**, **PC2**, and the copolymer site consisting of VP-VP-VP units have been calculated within the framework of density functional theory (DFT) with full optimization of the geometry of the initial molecules and their complexes using the Gaussian 09 program. The hybrid functional TPSSh and the 6-311++G**//6-31G* basic set were used as the method and basis. Using the polarized continuum model (PCM), an influence of the solvent (water) was taken into account. In the results of calculations, there are no imaginary oscillation frequencies, all the optimized structures correspond to the minimum potential energy. A similar approach has been already used by our research group (see, for example, [19, 20, 23]).

The cytotoxicity of the polymer nanoparticles and those bearing the Pt(IV) complex towards human cells was studied using HeLa cells (epithelioid carcinoma of the human uterine cervix, HeLa subline, M HeLa clone) obtained from the Russian collection of vertebrate cell cultures (Institute of Cytology, Russian Academy of Sciences, St. Petersburg). The cell cultivation was carried out according to the standard procedure in an atmosphere of 5% CO₂ at 37 °C in DMEM medium (PanEko, Russia) with the addition of 10% fetal calf serum (BioWest, France), NEAA (1%) (essential amino acids), penicillin (50 units·mL⁻¹), and streptomycin (50 μg·mL⁻¹).

The study of the cytotoxic properties of the PC compositions and copolymers was performed using the MTT test. The cells were seeded into 96-well culture plates at a concentration of 7×10⁴ cells/mL. The studied compounds were introduced into the culture medium in 24 h after sieving, *i.e.*, the culture medium was removed and replaced with that containing the copolymer, the copolymer with the encapsulated complex, or the initial PC. MTT dye (3-(4,5-dimethylthiazol-2-yl)-2,5-diphenyl-2H-tetrazolium bromide) was added to the incubation medium in 48 h after the introduction of the compounds. The resulting formazan crystals were dissolved in 100% DMSO. The optical density was measured at a fundamental wavelength of 570 nm and a background wavelength of 620 nm using a Spark 10M multifunctional microplate reader (Tecan, USA). The cytotoxicity index (IC₅₀) was determined based on the dose-dependent curves using a median effect analysis. The results of three independent experiments are presented as mean ± SD. The evaluation of statistical significance was performed using the *t*-test. The criterion of statistical significance was **p* < 0.05.

Conclusions

Based on the amphiphilic copolymers of *N*-vinylpyrrolidone, the nanostructures containing the Pt(IV) organic complexes, stable and soluble in aqueous neutral buffer media, were obtained that are known for their antitumor activity. It was shown that the copolymers suggested as the carriers and delivery vehicles are biocompatible and efficiently penetrate cells. Encapsulated complex **PC1** exhibited lower cytotoxicity towards A-172 cell line than the free complex at the same concentration. The platinum(IV) complexes encapsulated into

different copolymer particles demonstrated similar cytotoxicities. We assume that the Pt(IV) complex in this form will also show a decrease in the overall toxicity *in vivo* compared to the free compound.

Acknowledgements

This work was performed within the framework of State Tasks AAAA-A19-119071890015-6 and AAAA-A19-119061890019-5 using the equipment of the Multi-User Analytical Center at the Institute of Problems of Chemical Physics of the Russian Academy of Sciences.

The authors are thankful to N. V. Fadeeva, R. A. Manzhos, and E. I. Knerelman for the preparation of copolymers, CVA experiments, registration of the IR spectra, and helpful discussion.

Corresponding author

* E-mail: kurmaz@icp.ac.ru. Tel: +7(496)522-14-04 (V. A. Kurmaz)

References

- B. Rosenberg, L. Vancamp, J. E. Trosko, V. H. Mansour, *Nature*, **1969**, 222, 385–386. DOI: 10.1038/222385a0
- N. J. Wheate, S. Walker, G. E. Craig, R. Oun, *Dalton Trans.*, **2010**, 39, 8113–8127. DOI: 10.1039/c0dt00292e
- S. Dilruba, G. V. Kalayda, *Cancer Chemother. Pharmacol.*, **2016**, 77, 1103–1124. DOI: 10.1007/s00280-016-2976-z
- S. Schoch, V. Sen, W. Brenner, A. Hartwig, B. Köberle, *Biomedicines*, **2021**, 9, 1033. DOI: 10.3390/biomedicines9081033
- B. S. Fedorov, M. A. Fadeev, G. I. Kozub, S. M. Aldoshin, Z. G. Aliyev, L. O. Atovmnyan, N. P. Konovalova, T. E. Sashenkova, T. A. Kondrat'eva, S. V. Blokhina, *Pharm. Chem. J.*, **2009**, 43, 134–138. DOI: 10.1007/s11094-009-0256-5
- B. S. Fedorov, M. A. Fadeev, G. I. Kozub, A. N. Chekhlov, N. P. Konovalova, T. E. Sashenkova, E. I. Berseneva, O. V. Dobrokhotova, L. V. Tatyanyenko, *Russ. Chem. Bull.*, **2011**, 60, 1181–1184. DOI: 10.1007/s11172-011-0186-8
- V. D. Sen', V. V. Tkachev, L. M. Volkova, S. A. Goncharova, T. A. Raevskaya, N. P. Konovalova, *Russ. Chem. Bull.*, **2003**, 52, 421–426. DOI: 10.1023/A:1023475319835
- V. D. Sen', V. A. Golubev, G. V. Shilov, A. V. Chernyak, V. A. Kurmaz, V. B. Luzhkov, *J. Org. Chem.*, **2021**, 86, 3176–3185. DOI: 10.1021/acs.joc.0c02526
- V. D. Sen', A. A. Terentiev, N. P. Konovalova, in: *Nitroxides - Theory, Experiment and Applications*, A. I. Kokorin (Ed.), IntechOpen, London, **2012**, pp. 385–406. DOI: 10.5772/39113
- H. S. Oberoi, N. V. Nukolova, A. V. Kabanov, T. K. Bronic, *Adv. Drug Delivery Rev.*, **2013**, 65, 1667–1685. DOI: 10.1016/j.addr.2013.09.014
- E. A. Pashkina, L. V. Grishina, A. A. Aktanova, V. A. Kozlov, *Inorg. Chim. Acta*, **2021**, 522, 120370. DOI: 10.1016/j.ica.2021.120370
- E. V. Razuvaeva, K. T. Kalinin, N. G. Sedush, A. A. Nazarov, D. S. Volkov, S. N. Chvalun, *Mendeleev Commun.*, **2021**, 31, 512–514. DOI: 10.1016/j.mencom.2021.07.025
- A. K. Mandal, *Int. J. Polym. Mater. Polym. Biomater.*, **2021**, 70, 287–297. DOI: 10.1080/00914037.2020.1713780
- M. Kalomiraki, K. Thermos, N. Chaniotakis, *Int. J. Nanomed.*, **2016**, 11, 1–12. DOI: 10.2147/IJN.S93069
- R. M. Kannan, E. Nance, S. Kannan, D. A. Tomalia, *J. Intern. Med.*, **2014**, 276, 579–617. DOI: 10.1111/joim.12280
- S. A. Sorokina, I. Yu. Krasnova, *INEOS OPEN*, **2018**, 1, 85–93. DOI: 10.32931/iol1807r
- A. Agrawal, S. Kulkarni, *Int. J. Res. Dev. Pharm. Life Sci.*, **2015**, 4, 1700–1712.
- S. V. Kurmaz, V. D. Sen', A. V. Kulikov, D. V. Konev, V. A. Kurmaz, A. A. Balakina, A. A. Terent'ev, *Russ. Chem. Bull.*, **2019**, 68, 1769–1779. DOI: 10.1007/s11172-019-2623-z
- S. V. Kurmaz, N. V. Fadeeva, B. S. Fedorov, G. I. Kozub, N. S. Emel'yanova, V. A. Kurmaz, R. A. Manzhos, A. A. Balakina, A. A. Terentyev, *Mendeleev Commun.*, **2020**, 30, 22–24. DOI: 10.1016/j.mencom.2020.01.007
- S. V. Kurmaz, N. V. Fadeeva, V. M. Ignat'ev, V. A. Kurmaz, S. A. Kurochkin, N. S. Emel'yanova, *Molecules*, **2020**, 25, 6015. DOI: 10.3390/molecules25246015
- U. Koch, P. L. A. Popelier, *J. Phys. Chem.*, **1995**, 99, 9747–9754. DOI: 10.1021/j100024a016
- S. V. Kurmaz, V. Yu. Gak, V. A. Kurmaz, D. V. Konev, *Russ. J. Phys. Chem. A*, **2018**, 92, 329–333. DOI: 10.1134/S0036024418020152
- S. V. Kurmaz, N. V. Fadeeva, A. I. Gorshkova, S. A. Kurochkin, E. I. Knerelman, G. I. Davydova, V. I. Torbov, N. N. Dremova, V. A. Kurmaz, D. V. Konev, V. M. Ignatiev, N. S. Emel'yanova, *Materials*, **2021**, 14, 6757. DOI: 10.3390/ma14226757
- V. A. Kurmaz, A. S. Kotkin, G. V. Simbirtseva, *J. Solid State Electrochem.*, **2011**, 15, 2119. DOI: 10.1007/s10008-011-1534-1
- M. C. McCormick, K. Keijzer, A. Polavarapu, F. A. Schultz, M.-H. Baik, *J. Am. Chem. Soc.*, **2014**, 136, 8992–9000. DOI: 10.1021/ja5029765
- M. C. McCormick, F. A. Schultz, M.-H. Baik, *Polyhedron*, **2016**, 103, 28–34. DOI: 10.1016/j.poly.2015.09.040
- J. Leal, L. Santos, D. M. Fernández-Aroca, J. V. Cuevas, M. A. Martínez, A. Massaguer, F. A. Jalón, M. J. Ruiz-Hidalgo, R. Sánchez-Prieto, A. M. Rodríguez, G. Castañeda, G. Durá, M. C. Carrión, S. Barrabés, *J. Inorg. Biochem.*, **2021**, 218, 111403. DOI: 10.1016/j.jinorgbio.2021.111403
- M. H. Baik, F. Marken, A. Neudeck, A. M. Bond, in: *Electroanalytical Methods. Guide to Experiments and Applications*, F. Scholz (Ed.), Springer, Berlin, **2002**, pp. 57–106.
- L. M. Korotaeva, V. A. Kurmaz, T. Ya. Rubinskaya, V. P. Gul'tyai, *Russ. J. Electrochem.*, **2015**, 51, 1135–1148. DOI: 10.1134/S1023193515120083
- A. G. Krivenko, A. S. Kotkin, V. A. Kurmaz, *Russ. J. Electrochem.*, **2005**, 41, 137–153. DOI: 10.1007/s11175-005-0025-z
- D. V. Konev, K. V. Lizgina, D. K. Khairullina, M. A. Shamraeva, C. H. Devillers, M. A. Vorotyntsev, *Russ. J. Electrochem.*, **2016**, 52, 778–787. DOI: 10.1134/S1023193516060069
- Z. N. Gafurov, I. F. Sakhapov, V. M. Babaev, A. B. Dobrynin, V. A. Kurmaz, K. E. Metlushka, I. Kh. Rizvanov, G. R. Shaikhutdinova, O. G. Sinyashin, D. G. Yakhvarov, *Russ. Chem. Bull.*, **2017**, 66, 254–259. DOI: 10.1007/s11172-017-1725-8

This article is licensed under a Creative Commons Attribution-NonCommercial 4.0 International Licence.

